Electronic Supplementary Material (ESI) for New Journal of Chemistry.

Improved Plasmonic Au-Ag/TiO_2/rGO Photocatalyst through Entire Visible Range Absorption, Charge Separation and High Adsorption Ability.

Hicham Atout,[a,b] Abdellah Bouguettoucha,[b] Derradji Chebli,[b] Julián Crespo,[a] Jean-Charles Dupin,[c] José M. López-de-Luzuriaga,[a] Hervé Martínez,[c] Miguel Monge,*[,a] M. Elena Olmos,[a] María Rodríguez-Castillo[a]

ELECTRONIC SUPPLEMENTARY INFORMATION

[a.] *Dr. H. Atout, Dr. J. Crespo, Prof. J. M. López-de-Luzuriaga, Dr. M. Monge, Prof. M. E. Olmos, Dr. M. Rodríguez-Castillo*
Departmento de Química. Centro de Investigación en Síntesis Química (CISQ)
Universidad de La Rioja
CCT-Madre de Dios 53, 26006-Logroño (La Rioja). SPAIN
E-mail: miguel.monge@unirioja.es
[b.] *Dr. H. Atout, Prof. D. Chebli, Prof. A, Bouguettoucha*
[b]*Département de Génie des Procédés, Laboratoire de Génie des Procédés Chimiques, Faculté de Technologie, Université Ferhat Abbas, Sétif-1, 19000 Sétif, Algeria.*
[c.] *Dr. J.-C. Dupin, Prof. H. Martinez*
Université de Pau & Pays de l'Adour/ E2S UPPA, CNRS, Institut des Sciences Analytiques et de Physicochimie pour l'Environnement et les Matériaux, UMR5254, 64000, Pau, France

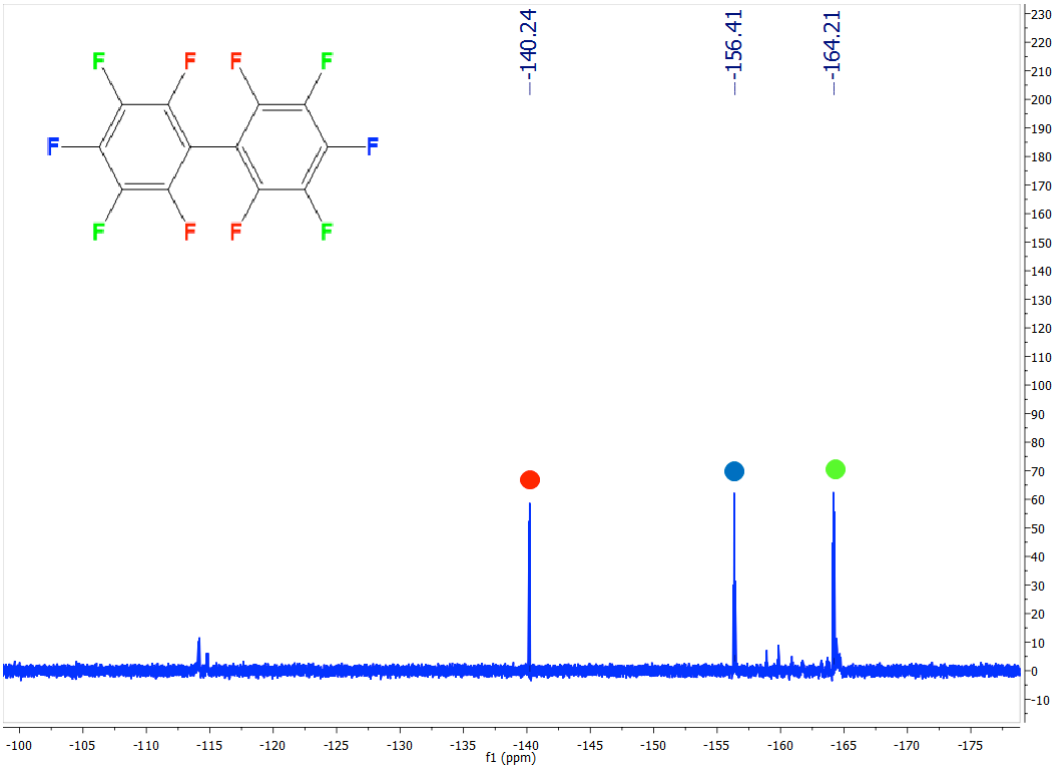

Figure S1. ^{19}F NMR spectra in d8-THF of the reaction by-product C_6F_5-C_6F_5 formed during the decomposition of complex $[Au_2Ag_2(C_6F_5)_4(OEt_2)_2]_n$ under reflux in the presence of PVP polymer, confirming a reductive elimination mechanism.

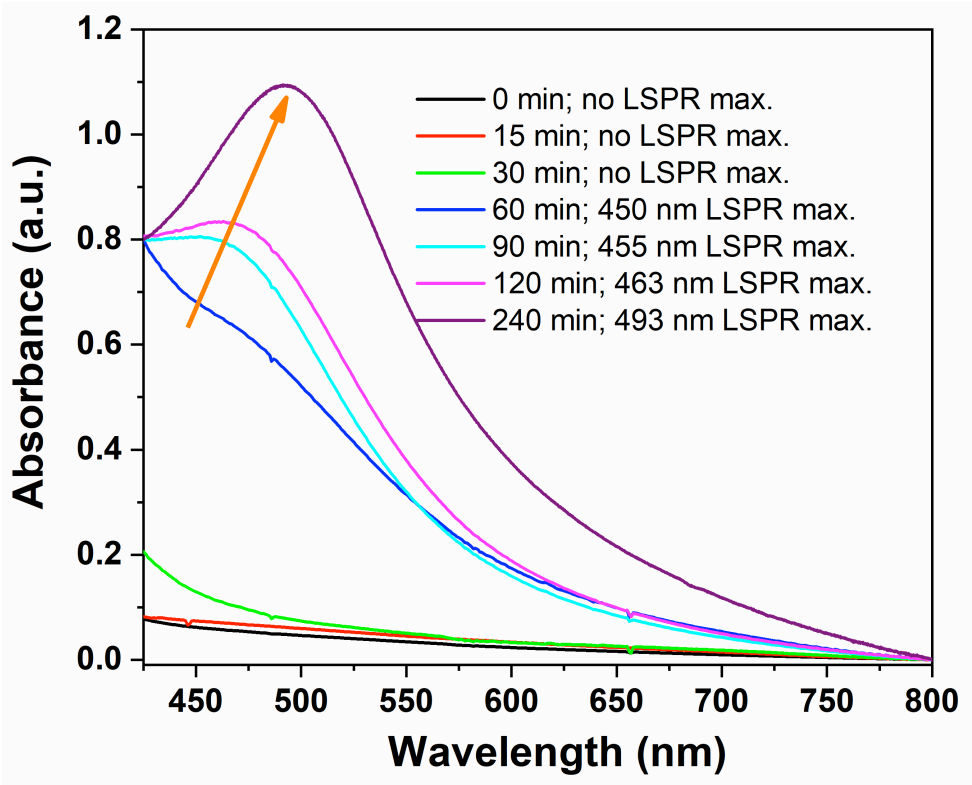

Figure S2. Time-resolved UV-Vis spectra of the AuAg-PVP NPs formation. The orange arrow shows the red-shift of the maximum absorption with time.

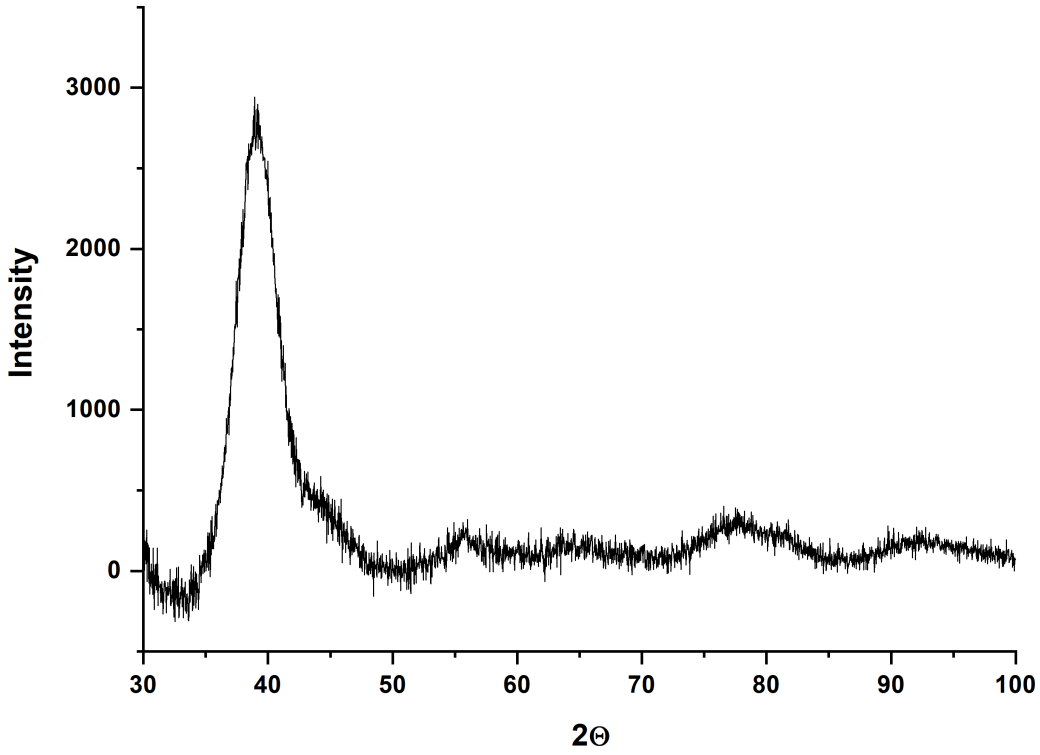

Figure S3. XRD spectrum of AuAg PVP NPs.

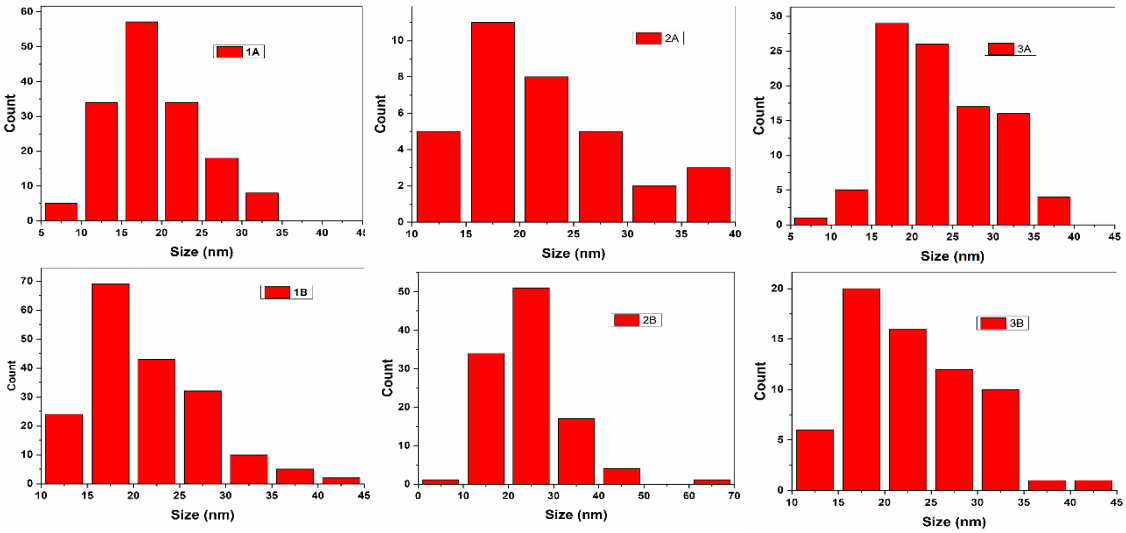

Figure S4. Size histograms of TiO_2 NPs in nanohybrids **1A**-**3A** (up) and **1B**-**3B** (bottom).

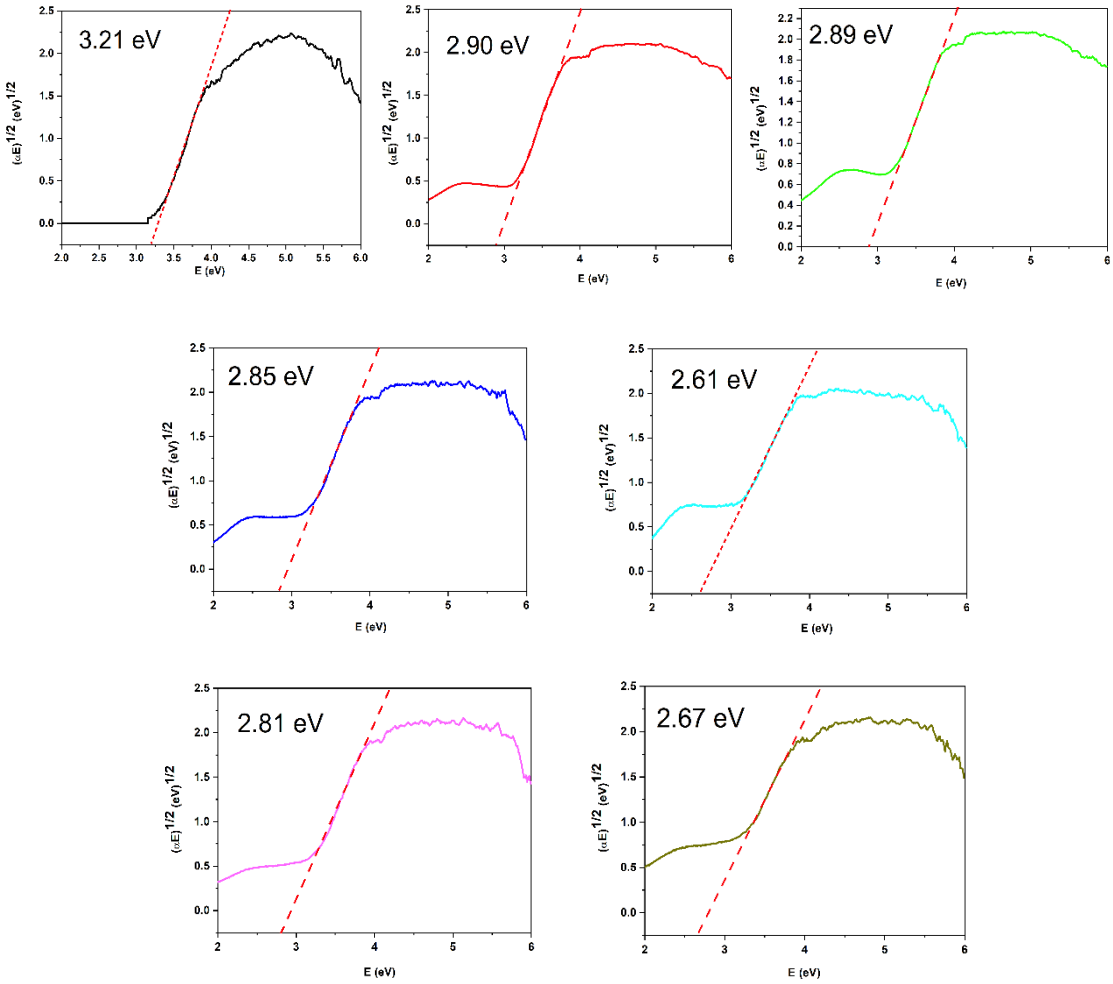

Figure S5. Tauc plots for solid samples of P25 TiO_2 NPs (black), **1A** (red), **1B** (green), **2A** (blue), **2B** (cyan), **3A** (magenta) and **3B** (ochre).

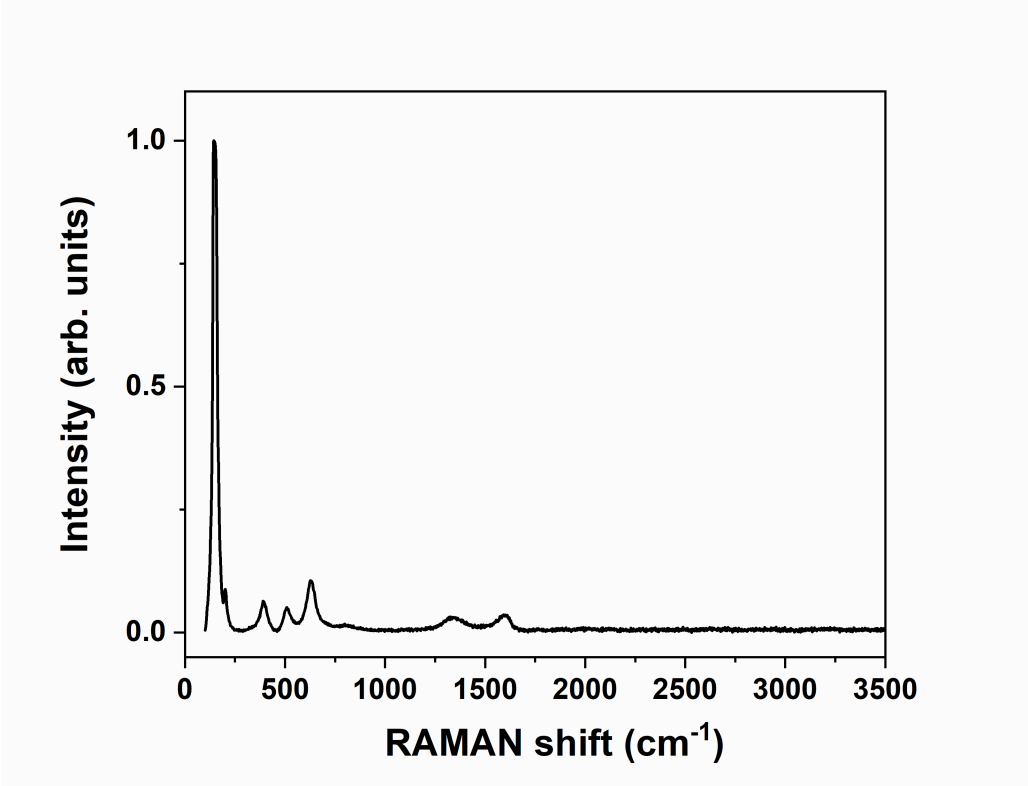

Figure S6. Raman spectrum for nanohybrid **3A**

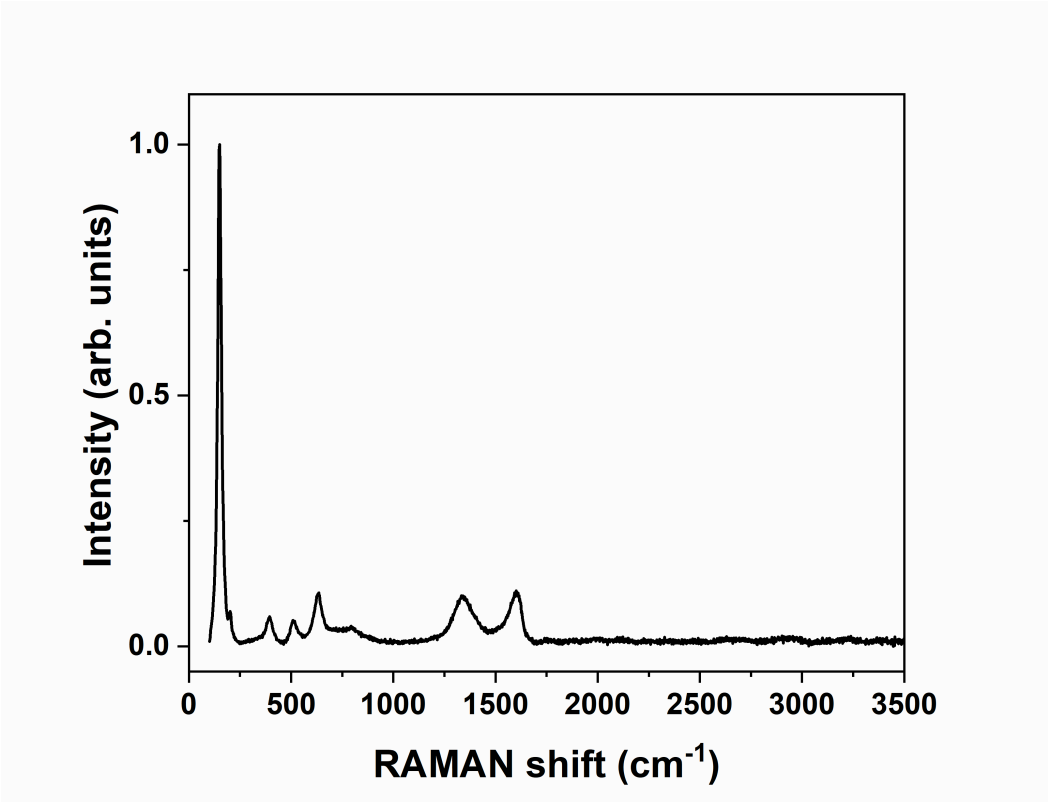

Figure S7. Raman spectrum for nanohybrid **3B**

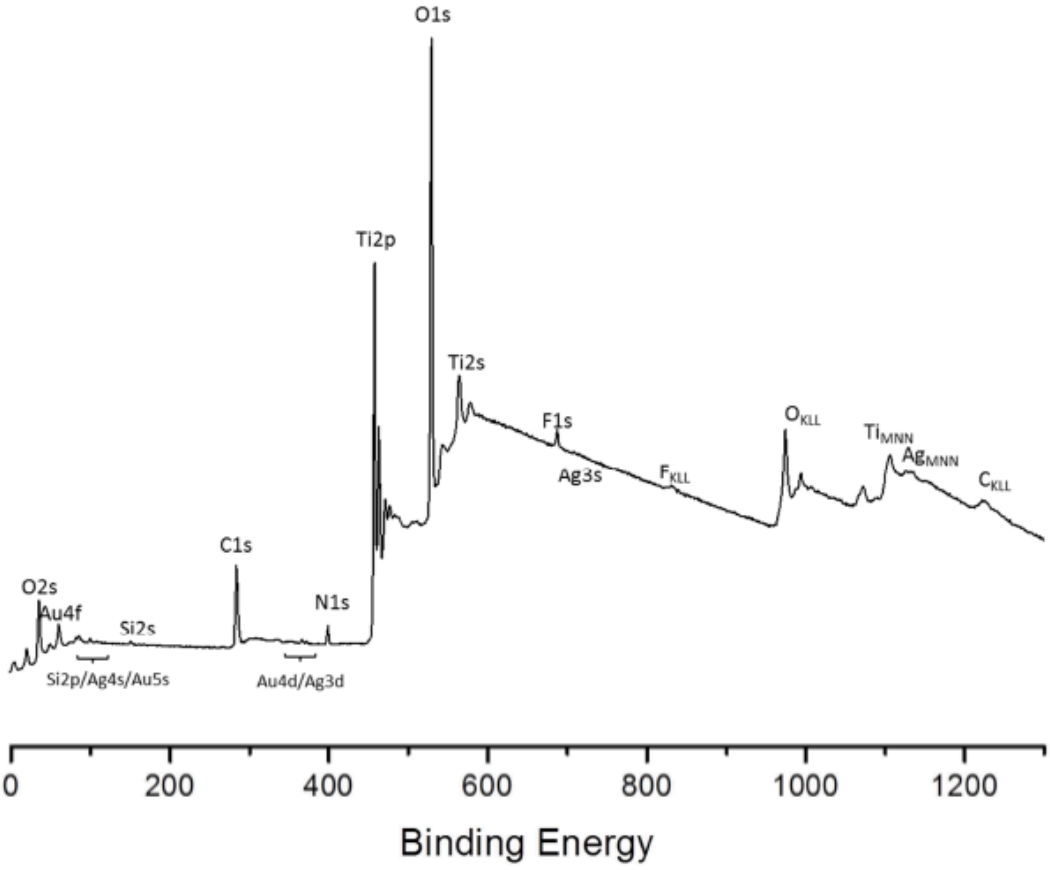

Figure S8. General XPS survey of AuAg-TiO_2 NP nanohybrid **1A**

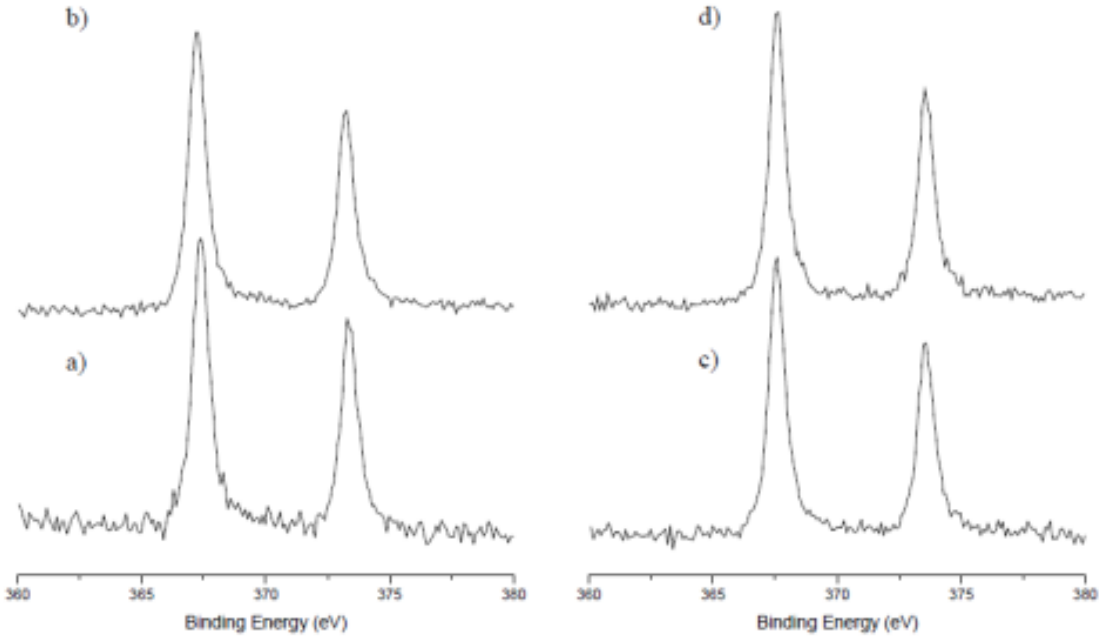

Figure S9. High-resolution $Ag_{3d5/2-3/2}$ XPS spectra of: **1A** (a), **1B** (b), **3A** (c) and **3B** (d) nanohybrids.

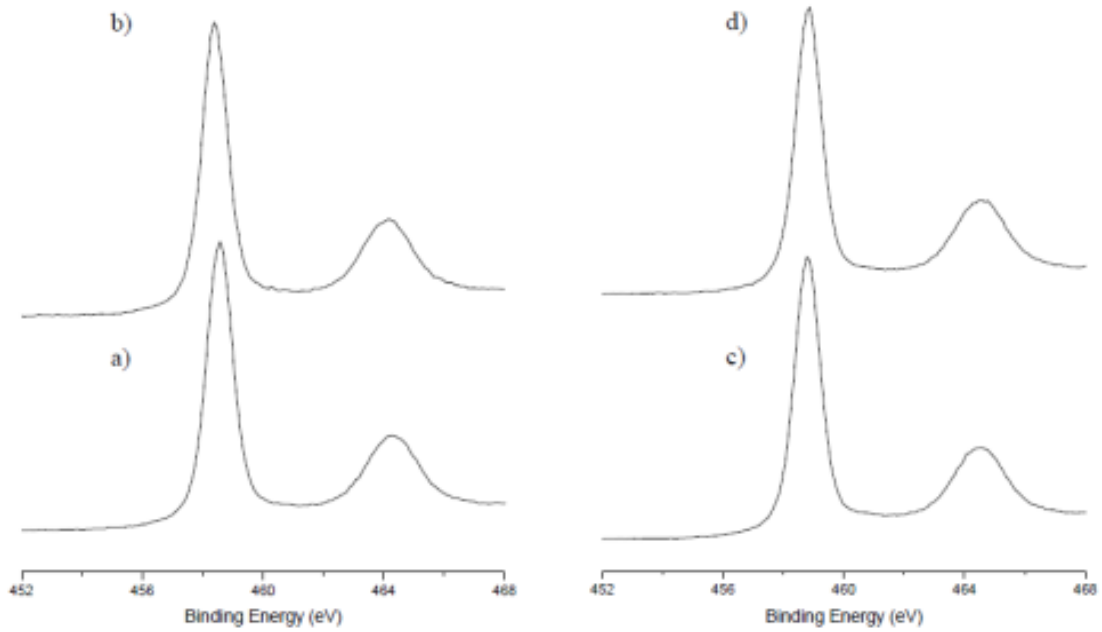

Figure S10. High-resolution $Ti_{2p3/2\text{-}1/2}$ XPS spectra of: **1A** (a), **1B** (b), **3A** (c) and **3B** (d) nanohybrids.

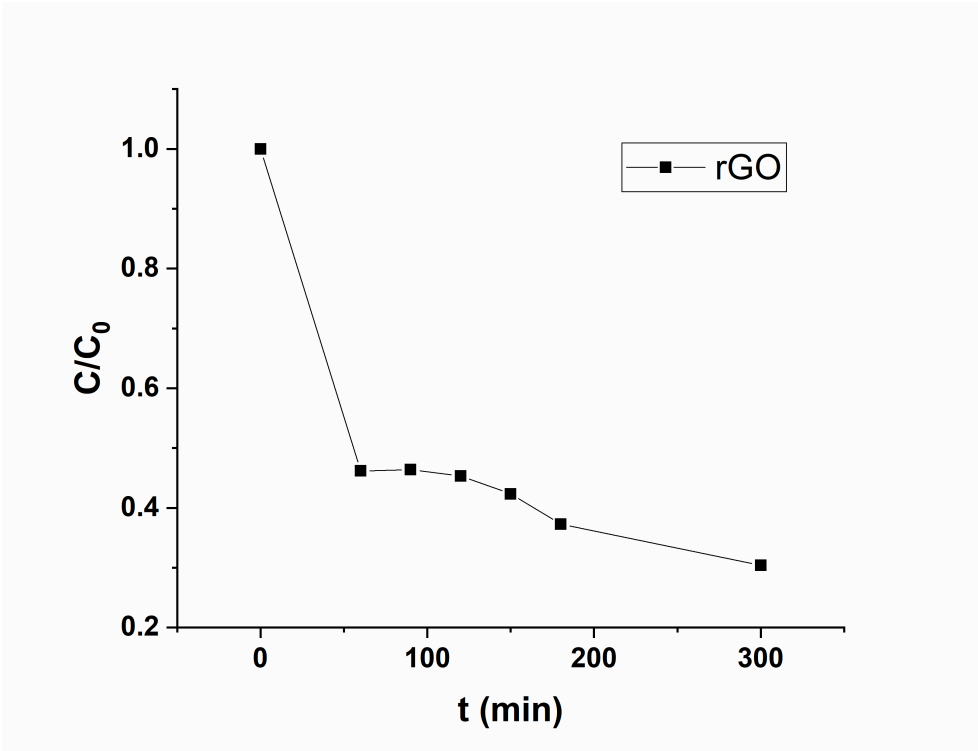

Figure S11. Adsorption of a methylene blue (MB) solution (5 mg/L concentration) under visible light (low-power white LED sources (4 x 10 W)) for a 2 mg sample of rGO.

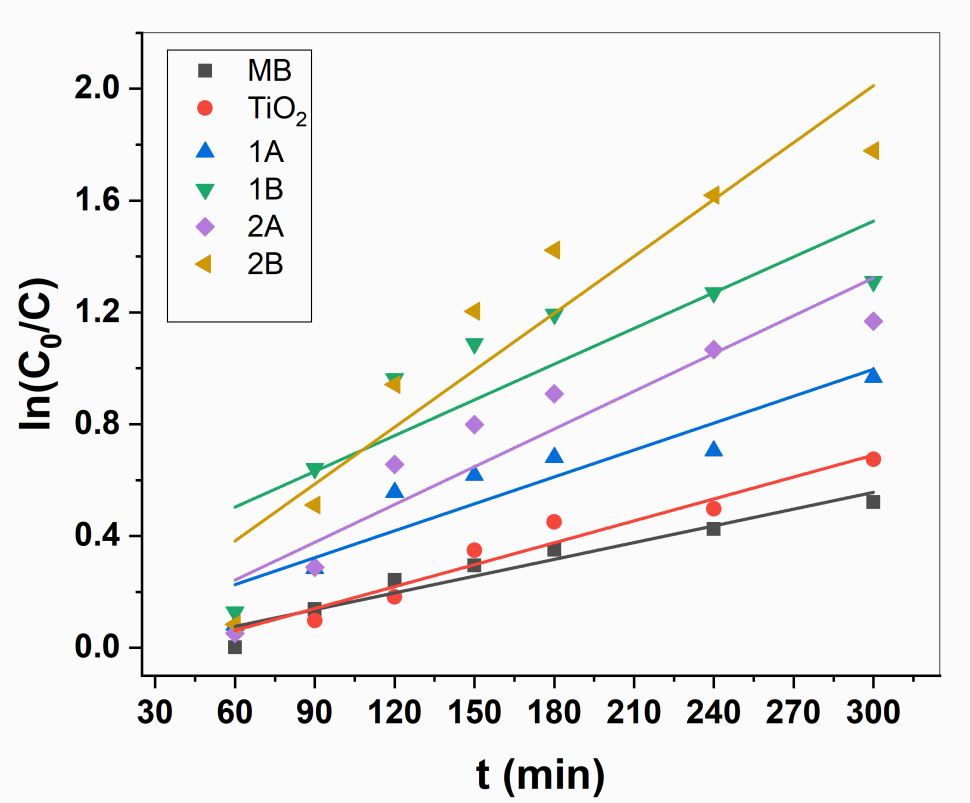

Figure S12. Kinetics of the photocatalysts (40 mg) under visible light. The fitting results are represented assuming a pseudo-first order reaction

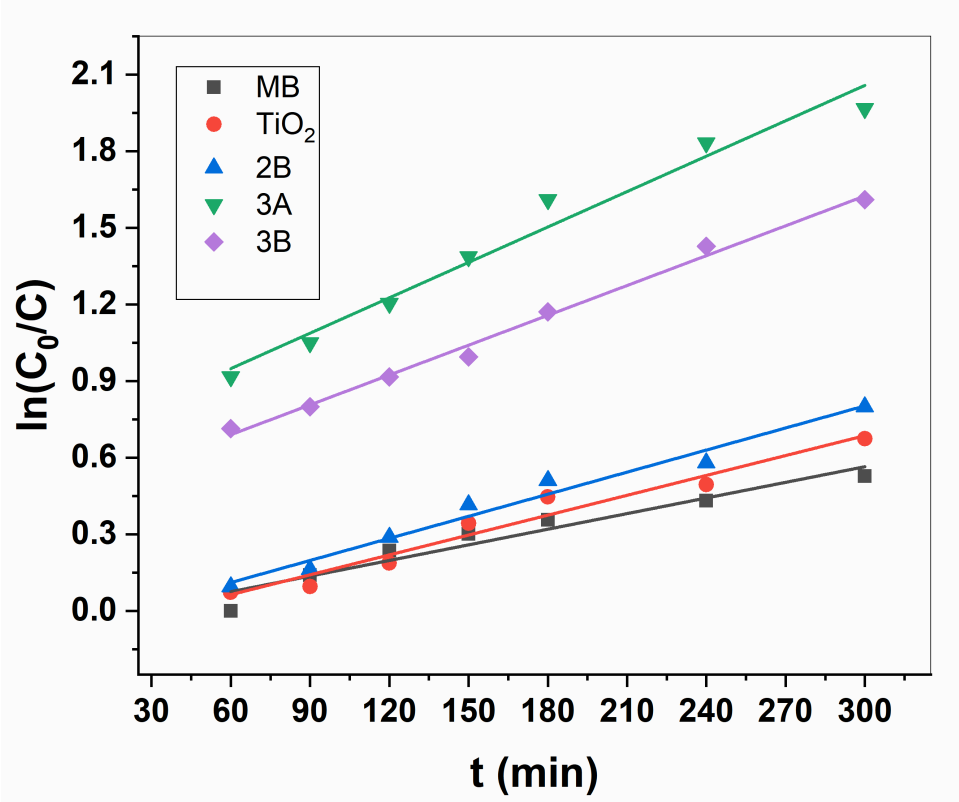

Figure S13. Kinetics of the photocatalysts (15 mg) under visible light. The fitting results are represented assuming a pseudo-first order reaction

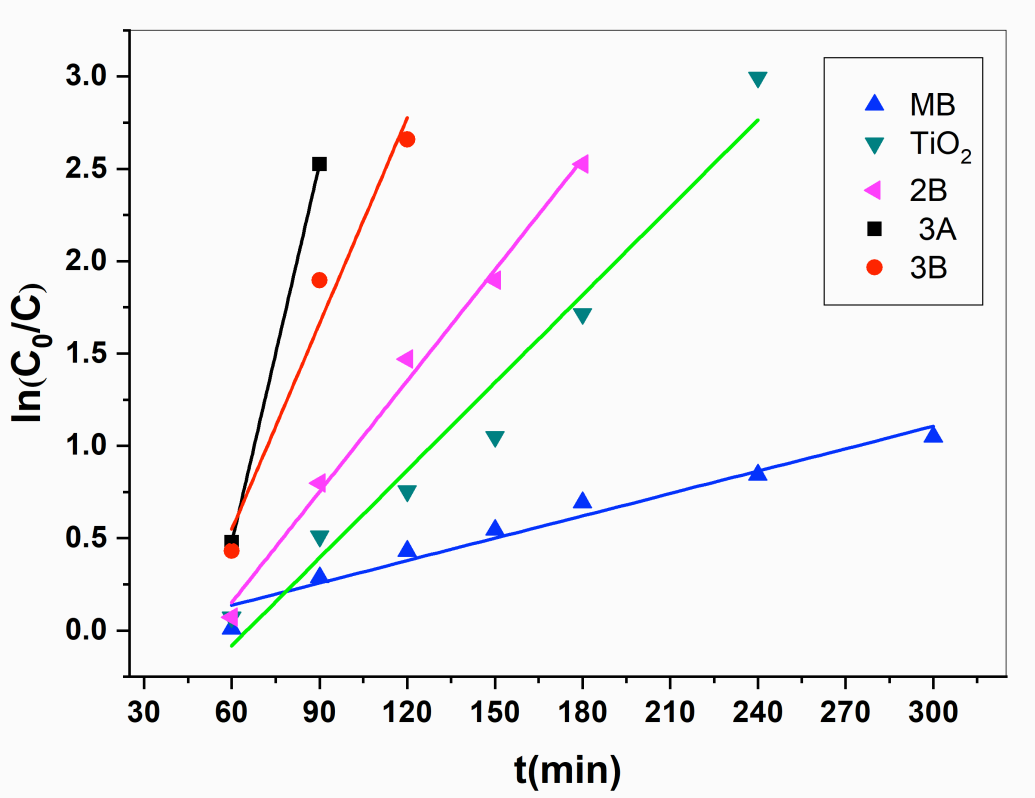

Figure S14. Kinetics of the photocatalysts (15 mg) under sunlight. The fitting results are represented assuming a pseudo-first order reaction